Fine-structured large deviations and the fluctuation theorem: Molecular motors and beyond

Patrick Pietzonka, Eva Zimmermann and Udo Seifert[(a)]

II. Institut für Theoretische Physik, Universität Stuttgart - 70550 Stuttgart, Germany

arXiv:1403.5987v1 [cond-mat.stat-mech] 24 Mar 2014

PACS 05.10.Gg – Stochastic analysis methods (Fokker-Planck, Langevin, etc.)
PACS 05.70.Ln – Nonequilibrium and irreversible thermodynamics
PACS 87.16.Nn – Motor proteins (myosin, kinesin, dynein)

Abstract –By extending large deviation theory to sub-exponential contributions, we determine the fine structure in the probability distribution of the observable displacement of a bead coupled to a molecular motor. More generally, for any stochastic motion along a periodic substrate, this approach reveals a discrete symmetry of this distribution for which hidden degrees of freedom lead to a periodic modulation of the slope typically associated with the fluctuation theorem. Contrary to previous interpretations of experimental data, the mean force exerted by a molecular motor is unrelated to the long-time asymptotics of this slope and must rather be extracted from its short-time limit.

For non-equilibrium steady states, the fluctuation theorem (FT) expresses a remarkable symmetry of the distribution function for entropy production as reviewed in [1]. Molecular motors [2,3] are one class of systems for which the FT has been explored. While early work concentrated on theoretical models [4–10], more recently the FT has been used to extract the torque exerted by motors like the F_1-ATPase from the distribution of displacements [11–13]. These experiments, however, have revealed that the FT is not naively applicable to this system since the characteristic slope derived from the FT shows a yet unexplained dependence on the length of the associated time intervals. Since, broadly speaking, the FT is valid in the long-time limit, the authors of [11,12] inferred the torque from the long-time asymptotics whereas, as we will show below, it is, in fact, given by the short-time limit.

The subtlety just mentioned is one manifestation of the role of hidden slow degrees of freedom that lead to deviations from the ideal FT symmetry [14–18]. While the theorem holds true for entropy production and, in simple models, also for displacement, it cannot naively be applied if relevant slow degrees of freedom are neglected. In the particular case of a molecular motor, the ignored degree of freedom is its state since the experimental data arise from a colloidal probe particle elastically linked to the not directly observable motor.

[(a)]E-mail: useifert@theo2.physik.uni-stuttgart.de

Large deviation theory can deal with rare fluctuations in the long-time limit as reviewed in [19]. In this letter, we refine large deviation theory in such a way that the "correct" slope characteristic for the FT in such situations with hidden degrees of freedom can be identified from data for the displacement. In fact, we can derive a more general discrete symmetry of this probability distribution for any stochastic motion along a spatially periodic structure. On a technical level, we have to determine the sub-exponential contributions to the large deviation function.

The basic idea of our approach is best illustrated using the arguably simplest model for a molecular motor subject to an external force transmitted by a probe particle as introduced in [20], where it was applied to model the measured efficiency of the F_1-ATPase [21,22]. The generalization to molecular motors with several substeps [23–30] will be given further below. In the one-step model shown in Fig. 1, the time-dependent position of the motor is given by a discrete variable $n(t)$ whereas the diffusive motion of the much larger, observable, bead is described by a continuous position $x(t)$. Each step of the motor covers the spatial distance d, such that the distance between the motor and the bead is $y(t) = n(t)d - x(t)$. The diffusive motion of the bead is governed by the Langevin-equation

$$\partial_t x(t) = [-f^{\mathrm{ex}} + \partial_y V(y) + \xi(t)]/\gamma. \tag{1}$$

It involves an external force f^{ex}, a force $\partial_y V(y)$ arising from the elastic linker with a potential energy

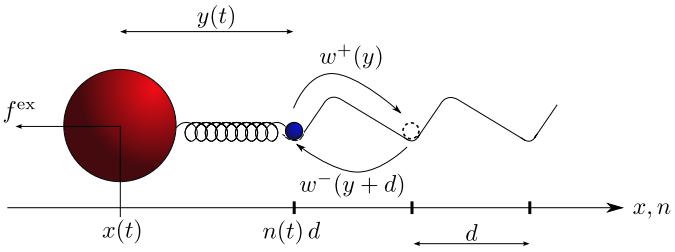

Fig. 1: Illustration of the one-step model. A bead (red) at position $x(t)$ is coupled to the motor (blue) at position $n(t)d$. The motor is a distance $y(t)$ ahead of the bead to which an external force f^{ex} is applied. The motor jumps at rates $w^{\pm}$ between adjacent minima of its (unresolved) periodic internal potential.

$V(y)$, and thermal noise $\xi(t)$ with the usual correlations $\langle\xi(t_1)\xi(t_2)\rangle = 2\gamma\delta(t_2-t_1)$ and γ the friction coefficient of the bead. Both Boltzmann's constant k_{B} and the temperature T are set to 1 throughout the letter thus making all energies dimensionless. The motor takes discrete forward and backward steps of length d at a rate $w^+(y)$ and $w^-(y)$, respectively. Each forwards step involves hydrolyzation of one ATP to ADP liberating $\Delta\mu$ of free energy and each backward step induces the reversed reaction. Both rates therefore depend implicitly on the concentrations of these molecules and on the instantaneous separation y. While the specific choice of forward and backward rate will be irrelevant for our main results, they have to obey the local detailed balance condition

$$w^+(y)/w^-(y+d) = \exp[\Delta\mu - V(y+d) + V(y)]. \tag{2}$$

The evolution of the probability $p(n,y,t)$ then follows the master equation

$$\partial_t p(n,y,t) = (L_1+L_2)p(n,y,t), \tag{3}$$

where

$$L_1 \equiv \partial_y[-f^{\mathrm{ex}} + \partial_y V(y)]/\gamma + \partial_y^2/\gamma \tag{4}$$

is the Fokker-Planck operator for motion of the bead and

$$\begin{aligned} L_2 p(n,y,t) \equiv &+ w^+(y-d)\,p(n-1,y-d,t) \\ &+ w^-(y+d)\,p(n+1,y+d,t) \\ &- [w^+(y)+w^-(y)]\,p(n,y,t) \end{aligned} \tag{5}$$

deals with the discrete jumps of the motor. As initial condition, we choose $p(n,y,0) = \delta_{n0}\,\delta(y-y_0)$. Note that the system as a whole, characterized by both n and y, does not reach a genuine non-equilibrium steady state, since we do not introduce periodic boundary conditions[1]. However, the marginal distribution for the elongation y reaches a stationary distribution $p^{\mathrm{s}}(y)$, from which we will later sample the initial value y_0.

[1]For rotary motors, like F_1-ATPase, x and n correspond to the accumulated number of revolutions.

The long-time limit can be analyzed by introducing the generating function [31]

$$g(\lambda,y,t) \equiv \sum_{n=-\infty}^{\infty} \mathrm{e}^{\lambda n} p(n,y,t), \tag{6}$$

which obeys $\partial_t g(\lambda,y,t) = \mathcal{L}(\lambda) g(\lambda,y,t)$ with

$$\begin{aligned} \mathcal{L}(\lambda)g(\lambda,y,t) \equiv &+ \mathrm{e}^{\lambda}\, w^+(y-d)\, g(\lambda,y-d,t) \\ &+ \mathrm{e}^{-\lambda}\, w^-(y+d)\, g(\lambda,y+d,t) \\ &+ [L_1 - w^+(y) - w^-(y)]\, g(\lambda,y,t) \end{aligned} \tag{7}$$

with initial condition $g(\lambda,y,0) = \delta(y-y_0)$.

The operator $\mathcal{L}(\lambda)$ has right eigenfunctions $q_i(\lambda,y)$ with eigenvalues $\alpha_i(\lambda)$. In the long-time limit, the largest eigenvalue (with label $i=0$) will dominate leading to

$$g(\lambda,y,t) \approx \mathrm{e}^{\alpha_0(\lambda)t} c_0(\lambda,y_0)\, q_0(\lambda,y) \equiv \mathrm{e}^{\alpha_0(\lambda)t} Q(\lambda,y,y_0). \tag{8}$$

The last definition combines the expansion coefficient c_0 through which the initial condition y_0 enters with the dominant eigenfunction q_0. Since $g(0,y,t)$ is the marginal distribution for y, we can identify $Q(0,y,y_0) = p^{\mathrm{s}}(y)$, which is, in fact, independent of y_0. From the generating function, the probability $p(n,y,t)$ can be recovered using the residue theorem in the complex $z \equiv \mathrm{e}^{\lambda}$ plane as

$$\begin{aligned} p(n,y,t) &= \frac{1}{2\pi\mathrm{i}} \oint \mathrm{d}z\, z^{-n-1} g(\ln z,y,t) \\ &= \frac{1}{2\pi\mathrm{i}} \int_{\lambda-\pi\mathrm{i}}^{\lambda+\pi\mathrm{i}} \mathrm{d}\lambda'\, \mathrm{e}^{-\lambda' n}\, g(\lambda',y,t) \\ &\approx \frac{1}{2\pi\mathrm{i}} \int_{\lambda-\pi\mathrm{i}}^{\lambda+\pi\mathrm{i}} \mathrm{d}\lambda'\, \mathrm{e}^{-\lambda' n + t\alpha_0(\lambda')} Q(\lambda',y,y_0) \end{aligned} \tag{9}$$

with $\lambda > 0$. A saddle point evaluation of this integral through λ obeying

$$\alpha_0'(\lambda) = n/t \equiv u \tag{10}$$

yields

$$p(n,y,t|y_0) \approx \mathrm{e}^{-th(n/t)} Q(\lambda(n/t),y,y_0)/\sqrt{2\pi t \alpha_0''(\lambda(n/t))} \tag{11}$$

where $'$ denotes a derivative with respect to λ from now on. The exponential term corresponds to the familiar large deviation form with the rate function given by the Legendre transformation of $\alpha_0(\lambda)$ according to

$$h(u) \equiv u\lambda(u) - \alpha_0(\lambda(u)) \tag{12}$$

which implies

$$\partial_u h(u) = \lambda(u). \tag{13}$$

The fine structure beyond the large deviation term arises from the remaining factors in (11). We first focus on n values of order 1 which for large t occur with an exponentially small probability. Still, these values will be

relevant for the fluctuation theorem. Expanding the exponent in (11) to first order in n/t and then setting $n/t \approx 0$ everywhere leads to

$$p(n,y,t|y_0) \approx \mathrm{e}^{-th(0)-\lambda_0 n} Q(\lambda_0,y,y_0)/\sqrt{2\pi t \alpha_0''(\lambda_0)} = f(t,0)\mathrm{e}^{-\lambda_0 n} Q(\lambda_0,y,y_0) \quad (14)$$

where $\lambda_0 \equiv \lambda(0)$ is the λ-value solving $\alpha_0'(\lambda) = 0$. The time-dependence is abbreviated by

$$f(t,u) \equiv \mathrm{e}^{-th(u)}/\sqrt{2\pi t \alpha_0''(\lambda(u))}. \quad (15)$$

The value λ_0 can be determined analytically since the convex $\alpha_0(\lambda)$ obeys, as will be shown in the general framework below, the Gallavotti-Cohen symmetry [8,9,32]

$$\alpha_0(\lambda) = \alpha_0(-\lambda - (\Delta\mu - f^{\mathrm{ex}}d)), \quad (16)$$

which implies

$$\lambda_0 = -(\Delta\mu - f^{\mathrm{ex}}d)/2. \quad (17)$$

Note that $-2\lambda_0$ corresponds to the entropy production in the medium associated with a displacement of motor and bead along one periodicity interval since $\Delta\mu$ is the input of chemical work and $f^{\mathrm{ex}}d$ is the delivered mechanical work. This entropy production is positive in the regime of interest $f^{\mathrm{ex}}d < \Delta\mu$.

For the experiments addressing the FT the relevant quantity is the probability distribution $p(\Delta x)$ for the distance

$$\Delta x \equiv n(t) + [y_0 - y(t)]/d \quad (18)$$

traveled by the bead during time t and measured in units of d. This distribution is obtained by summing $p(n,y,t|y_0)$ over all n and integrating over all initial y_0 with the stationary distribution $p^{\mathrm{s}}(y_0)$ as

$$p(\Delta x,t) = \int_{-\infty}^{\infty} \mathrm{d}y_0\, p^{\mathrm{s}}(y_0) \times \sum_n p(n, y = (n-\Delta x)d + y_0, t|y_0). \quad (19)$$

Plugging in (14) and suppressing the overall time dependence by defining $\mathcal{P}(\Delta x) \equiv \lim_{t\to\infty} p(\Delta x,t)/f(t,0)$ gives the asymptotically exact (unnormalized) distribution

$$\mathcal{P}(\Delta x) = \int_{-\infty}^{\infty} \mathrm{d}y_0\, p^{\mathrm{s}}(y_0) \times \sum_n \mathrm{e}^{-\lambda_0 n} Q(\lambda_0, (n-\Delta x)d + y_0, y_0). \quad (20)$$

While an explicit evaluation requires numerics as presented below, the crucial symmetry

$$\mathcal{P}(\Delta x + m) = \mathrm{e}^{-\lambda_0 m}\mathcal{P}(\Delta x) \quad (21)$$

for integer m is easily proven by shifting the summation index n.

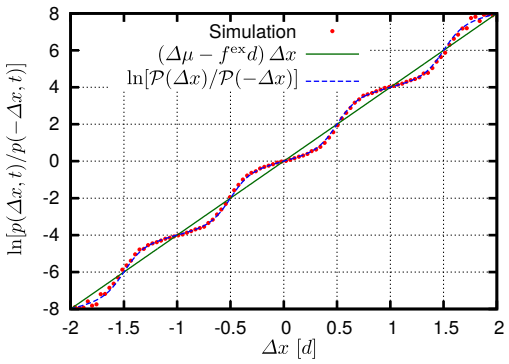

Fig. 2: FT-type representation of the long-time asymptotics of the distribution function $\ln[\mathcal{P}(\Delta x)/\mathcal{P}(-\Delta x)]$ (blue dashed line) compared to $\ln[p(\Delta x,t)/p(-\Delta x,t)]$ from simulations of (1) for $t = 1\,\mathrm{sec}$. The straight green line shows the slope corresponding to entropy production. Parameters: $\gamma = 0.41\,\mathrm{sec}/d^2$, $\Delta\mu = 19$, $f^{\mathrm{ex}} = 15/d$, $V(y) = (25/2)(y/d)^2$, $w^+(y) = 1\,575\,\mathrm{e}^{-2.5y/d}\,\mathrm{sec}^{-1}$, $w^-(y)$ determined from (2).

This discrete symmetry of the probability distribution for the displacement of the bead is our first main result. It is valid in the long-time limit for all $|\Delta x|$ of order 1, i.e., for values of $|\Delta x|$ that do not scale with time t. It implies that this distribution can be written in the form

$$\mathcal{P}(\Delta x) = \mathrm{e}^{-\lambda_0 \Delta x}\phi(\Delta x) \quad (22)$$

with a periodic function $\phi(\Delta x + 1) = \phi(\Delta x)$, and, in particular $\phi(-1/2) = \phi(1/2)$. The latter form implies for the FT-type representation

$$\lim_{t\to\infty} \ln \frac{p(\Delta x,t)}{p(-\Delta x,t)} = \ln \frac{\mathcal{P}(\Delta x)}{\mathcal{P}(-\Delta x)} = -2\lambda_0 \Delta x + \psi(\Delta x) \quad (23)$$

with a periodic antisymmetric function $\psi(\Delta x) \equiv \ln[\phi(\Delta x)/\phi(-\Delta x)]$ that vanishes if Δx is evaluated at integer or half integer positions. Hence, the "slope" in such an FT-like representation of the distance traveled by the bead is not constant but rather periodically modulated around the value corresponding to entropy production. In particular, the slope at $\Delta x = 0$ is *not* given by the entropy production. However, the slope evaluated as a finite difference over an integer interval chosen symmetrically around $\Delta x = 0$ allows to infer the correct entropy production. In Fig. 2, we illustrate this result by comparing simulations of this model with an explicit calculation of these fine-structured large deviations via a straightforward numerical evaluation of the largest eigenvalue $\alpha_0(\lambda_0)$, the corresponding eigenfunction $q_0(\lambda_0,y)$, the expansion coefficient $c_0(\lambda_0,y_0)$ and the stationary distribution $p^{\mathrm{s}}(y_0)$ for realistic parameters as derived in [20]. Even for the small value $t = 1\,\mathrm{sec}$, the FT representation of the probability distribution $p(\Delta x,t)$ is already in excellent agreement with the numerically calculated $\mathcal{P}(\Delta x)$ for the long-time limit. As expected, intersections with the straight line corresponding to entropy production occur at integer and half-integer values of Δx.

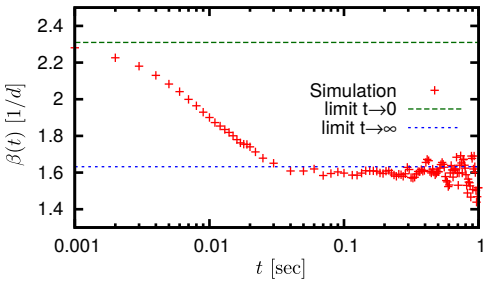

Fig. 3: Time dependence of the FT-slope $\beta(t)$ (24). While the short-time limit corresponds to the mean force exerted on the bead (green line at $\langle \partial_y V(y)\rangle - f^{\mathrm{ex}} = 2.31/d$), the long-time limit has no physical interpretation beyond being the slope of the FT representation of $\mathcal{P}(\Delta x)$ at $\Delta x = 0$ (blue line at $1.63/d$). Parameters as in Fig. 2.

The average force $\langle \partial_y V(y)\rangle$ that the motor exerts on the bead that has tentatively been identified with the long-time limit value of the slope

$$\beta(t) \equiv \lim_{\Delta x\to 0} \frac{1}{\Delta x\, d} \ln \frac{p(\Delta x, t)}{p(-\Delta x, t)} \tag{24}$$

at $\Delta x = 0$ in [11, 12] is rather given by the short-time limit of this slope as we now show. For short times t, the distribution of displacements of the bead corresponds to a diffusion biased by a force $F(y_0) \equiv -f^{\mathrm{ex}} + \partial_y V(y)|_{y_0}$. Taking the steady state average over the initial y_0 yields

$$p(\Delta x, t) \approx \int_{-\infty}^{\infty} \mathrm{d}y_0\, \frac{p^{\mathrm{s}}(y_0)}{d\sqrt{4\pi t/\gamma}}\, \mathrm{e}^{-(\Delta x d - F(y_0)t/\gamma)^2\gamma/(4t)}. \tag{25}$$

Simple calculus then shows that

$$\lim_{t\to 0} \beta(t) = -f^{\mathrm{ex}} + \int_{-\infty}^{\infty} \mathrm{d}y_0\, p^{\mathrm{s}}(y_0)\, \partial_y V(y_0) \tag{26}$$

which indeed involves the mean force the motor exerts on the bead. Simulations of the full model (see Fig. 3) confirm the validity of this simple derivation.

For the rest of the letter, we return to the long-time limit. A fine structure as presented above is not confined to a region around $n \simeq \Delta x \simeq O(1)$. We can choose any coarse scale $n_{\mathrm{c}} = ut$. The choice $u = 0$ is what we have just discussed whereas $u = v$ with v the mean velocity of the motor (or bead) would correspond to the maximum of the distribution. As sketched in Fig. 4, we can then zoom in on a finer scale of order 1 around $n_{\mathrm{c}} = ut$ to get

$$p_u(n, y, t|y_0) \approx f(t, u)\, \mathrm{e}^{-\lambda_u(n-n_{\mathrm{c}})}\, Q(\lambda_u, y, y_0) \tag{27}$$

where λ_u solves $\alpha_0'(\lambda_u) = u$. The index u at p_u indicates that this result for the fine structure of the distribution is valid for values of n that deviate $O(1)$ from the growing coarse scale $n_{\mathrm{c}} = ut$. For the probability distribution of

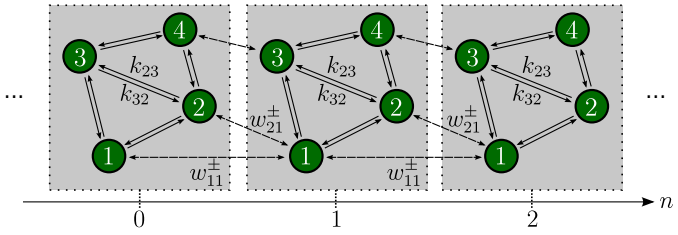

Fig. 5: Generalized network. Each square box is a mesostate containing a set of microstates (green circles). The mesostates repeat periodically and are labeled by the index n. Transition rates k_{ij} apply within one mesostate and the rates $w_{ij}^{\pm}$ refer to transitions between adjacent mesostates.

displacements, we obtain in the long-time limit

$$\begin{aligned}\mathcal{P}_u(\Delta x|y_0) &\equiv \lim_{t\to\infty} \sum_n p_u(n, (n-\Delta x)d + y_0, t|y_0)/f(u,t) \\ &= \sum_n \mathrm{e}^{-\lambda_u(n-n_{\mathrm{c}})} Q(\lambda_u, (n-\Delta x)d + y_0, y_0)\end{aligned} \tag{28}$$

similarly to (20), as shown in the small panels of Fig. 4. As above, the discrete symmetry

$$\mathcal{P}_u(\Delta x + m|y_0) = \mathrm{e}^{-\lambda_u m}\mathcal{P}_u(\Delta x|y_0) \tag{29}$$

holds for both m and $|\Delta x - ut|$ of order 1.

This approach can easily be generalized to any model with spatial periodicity, see Fig. 5. The states are grouped into identical mesostates labeled by n. Each mesostate consists of the same set of microstates labeled by i. The state of the system is thus given by the pair (n, i) which occurs with probability $p(n, i, t)$. Transitions between the microstates are possible only if both microstates belong either to the same mesostate or to an adjacent one. For the first case, the rate from (n, i) to (n, j) is given by k_{ij}. The transition rates from (n, i) to $(n+1, j)$ are given by w_{ij}^{+} and those from $(n+1, j)$ to (n, i) are given by w_{ij}^{-}. The spatial periodicity implies that none of the rates depends on n. A bead attached to a motor is covered by this more general set-up if its continuous position y is discretized.

These rates imply that the evolution of the generating function

$$g_i(\lambda, t) \equiv \sum_n \mathrm{e}^{\lambda n} p(n, i, t) \tag{30}$$

is given by

$$\begin{aligned}\partial_t g_i(\lambda, t) &= \sum_j \left[k_{ji} + \mathrm{e}^{\lambda} w_{ji}^{+} + \mathrm{e}^{-\lambda} w_{ij}^{-} - r_i\delta_{ij}\right] g_j(\lambda, t) \\ &\equiv \sum_j \mathcal{L}_{ij}(\lambda)\, g_j(\lambda)\end{aligned} \tag{31}$$

with the exit rate $r_i \equiv \sum_\ell (w_{i\ell}^{+} + w_{\ell i}^{-} + k_{i\ell})$.

The matrix $\mathcal{L}_{ij}(\lambda)$ has eigenvalues $\alpha_\nu(\lambda)$, with $\alpha_0(\lambda)$ denoting the largest one, and right eigenvectors $q_{\nu i}(\lambda)$ obeying

$$\sum_j \mathcal{L}_{ij}(\lambda)\, q_{\nu j}(\lambda) = \alpha_\nu(\lambda)\, q_{\nu i}(\lambda). \tag{32}$$

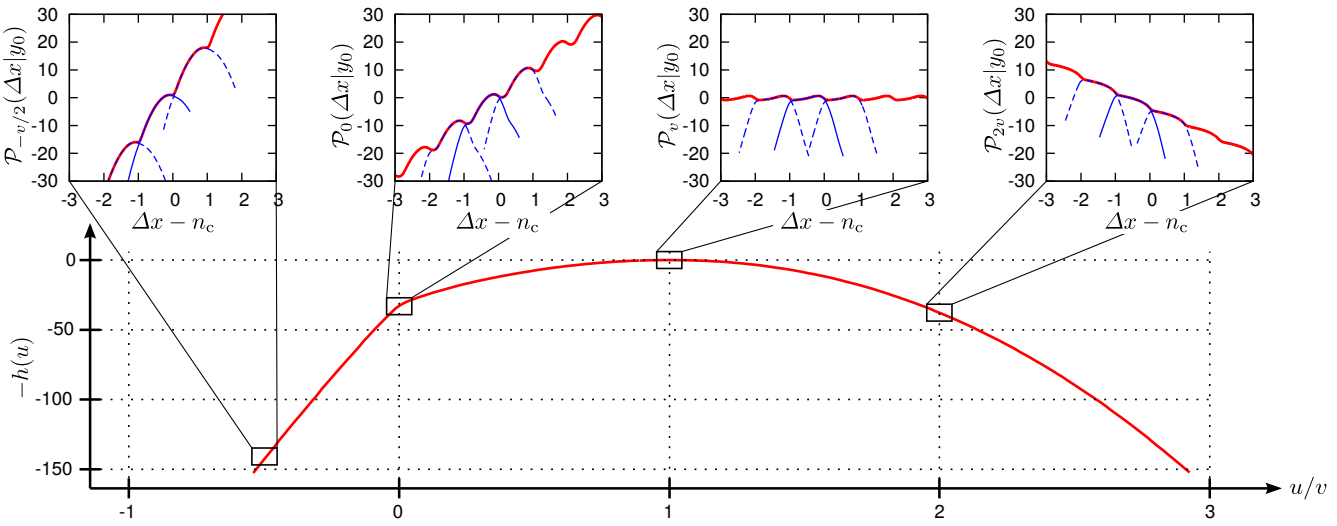

Fig. 4: Illustration of the properties of the long-time limit of the distribution $p_u(n, y, t|y_0)$. The large panel shows the exponential contributions through the rate function $-h(u)$. The small panels show the sub-exponential contributions $\mathcal{P}_u(\Delta x|y_0)$ for selected values of u and $y_0 = 0$ (red curves). The blue curves show the eigenfunctions in the form $\mathrm{e}^{-\lambda_u m} Q(\lambda_u, (n_c + m - \Delta x)d, 0)$ for $m = 0$ (solid) and $m = \pm 1$ (dashed). Parameters: $\Delta\mu = 19$, $f^{\mathrm{ex}} = 0$, $V(y) = 20(y/d)^2$, $\gamma = 1\,\mathrm{sec}/d^2$, $w^+(y) = 595\,\mathrm{e}^{-4y/d}\,\mathrm{sec}^{-1}$.

Each eigenvalue α_ν also comes with a left eigenvector $\tilde{q}_{\nu i}(\lambda)$

$$\sum_i \tilde{q}_{\nu i}(\lambda)\, \mathcal{L}_{ij}(\lambda) = \alpha_\nu(\lambda)\, \tilde{q}_{\nu j}(\lambda) \tag{33}$$

with the inner product

$$\sum_i \tilde{q}_{\nu i}(\lambda)\, q_{\mu i}(\lambda) = C_\nu(\lambda)\, \delta_{\nu\mu}. \tag{34}$$

In the long-time limit, the generating function becomes

$$g_i(\lambda, t) \approx \mathrm{e}^{\alpha_0(\lambda)t} c_0(\lambda, i_0)\, q_{0i}(\lambda). \tag{35}$$

If the system starts at time $t = 0$ in $(0, i_0)$, the expansion coefficient is given by $c_0(\lambda, i_0) = \tilde{q}_{0i_0}(\lambda)/C_0(\lambda)$.

The fine structure around $n_c = ut$ follows by repeating the same steps as above as

$$\begin{aligned} p_u(n, i, t|i_0) &\approx \mathrm{e}^{-th(u)-(n-n_c)\lambda_u}\, \frac{\tilde{q}_{0i_0}(\lambda_u)\, q_{0i}(\lambda_u)}{C_0(\lambda_u)\sqrt{2\pi t \alpha_0''(\lambda_u)}} \\ &= f(t, u)\, \mathrm{e}^{-\lambda_u(n-n_c)}\, Q(\lambda_u, i, i_0) \end{aligned} \tag{36}$$

with

$$Q(\lambda_u, i, i_0) \equiv \tilde{q}_{0i_0}(\lambda_u)\, q_{0i}(\lambda_u)/C_0(\lambda_u), \tag{37}$$

which contains the initial microstate i_0. This relation implies that for fixed initial and final states i_0, i, the probability for observing different n's around the coarse scale $n_c = ut$ obeys

$$\mathcal{P}_u(n + m, i|i_0) = \mathrm{e}^{-\lambda_u m} \mathcal{P}_u(n, i|i_0), \tag{38}$$

where we suppress again the time dependence by writing $\mathcal{P}_u(\cdot) \equiv \lim_{t\to\infty} p_u(\cdot, t)/f(u, t)$. As the introductory model has shown, in an experiment, restricting the average to fixed i and i_0 may be unrealistic as the direct observation of $n(t)$ might be. For a general observable defined as

$$\Delta x(t) \equiv n(t) + z_i(t) - z_{i_0} \tag{39}$$

that associates a real variable z_i (like displacement) to each microstate i, we get as above for the fine-structured distribution around the coarse scale $n_c = ut$

$$p_u(\Delta x, t) = \sum p^{\mathrm{s}}(i_0)\, p(n, i, t|i_0) \tag{40}$$

where $p^{\mathrm{s}}(i_0)$ is the stationary distribution. In the long-time limit, we have

$$\mathcal{P}_u(\Delta x) = \sum p^{\mathrm{s}}(i_0)\, \mathrm{e}^{-\lambda_u n} Q(\lambda_u, i, i_0) \tag{41}$$

where the sums runs over all n, i, i_0 with $\Delta x(n, i, i_0) = \Delta x$. As above, the summation implies the discrete symmetry

$$\mathcal{P}_u(\Delta x + m) = \mathrm{e}^{-\lambda_u m} \mathcal{P}_u(\Delta x), \tag{42}$$

and, for $u = 0$, the modulated FT (23).

The discrete symmetry thus derived for a general spatially periodic model and the identification of a properly discretized slope with λ_0 is universally valid. The identification of this slope with genuine entropy production, however, requires that any cycle either within a mesostate or involving several mesostates comes with zero entropy production. If this condition is violated, entropy production without concomitant displacement occurs. Formally, this condition means, first, that the rates within each mesostate must obey the detailed balance condition

$$k_{ij}/k_{ji} = \mathrm{e}^{\Phi_i - \Phi_j}. \tag{43}$$

The generalized potential Φ comprises not only the internal energy of the system but also external contributions like displacement against an external force or the

consumption of molecules associated with a fixed chemical potential [29]. Second, the rates between adjacent mesostates must fulfill

$$w_{ij}^{+}/w_{ij}^{-} = \mathrm{e}^{\Phi_i - \Phi_j + \Delta S} \tag{44}$$

with ΔS independent of i and j. Straightforward algebra then shows

$$\mathrm{e}^{-\Phi_i}\mathcal{L}_{ji}(\lambda)\,\mathrm{e}^{\Phi_j} = \mathcal{L}_{ij}(-\lambda - \Delta S). \tag{45}$$

Hence, $\mathcal{L}(\lambda)$ and $\mathcal{L}(-\lambda - \Delta S)$ have the same spectrum which implies the Gallavotti-Cohen symmetry

$$\alpha_0(\lambda) = \alpha_0(-\lambda - \Delta S) \tag{46}$$

and the relation $\mathrm{e}^{-\Phi_i}\tilde{q}_{\nu i}(\lambda) = q_{\nu i}(-\lambda - \Delta S)$ between the left and right eigenvectors. From (46) the fluctuation theorem-type relation

$$h(u) = h(-u) - u\Delta S \tag{47}$$

follows for the rate function $h(u)$. In this case, $\Delta S = -2\lambda_0$ indeed corresponds to the entropy production associated with stepping one periodicity unit. This insight can be turned into a simple experimental check for the presence of idle cycles that burn ATP without leading to net displacement [33–36]. If, in the long-time limit, the properly discretized slope in the FT representation of the displacement deviates from $\Delta\mu - f^{\mathrm{ex}}d$, then the motor must have idle cycles.

Colloidal particles either driven externally over periodic potentials [37, 38] or subject to active motion along periodic substrates [39] are a second class of systems for which the present approach could lead to a refined picture. A particularly intriguing observation in the first case was the occurrence of a kink around zero entropy production [40–42], also visible here in Fig. 4. It will also be interesting to explore within this approach the deviations from the ideal FT observed experimentally in such systems [16].

In conclusion, we have introduced the concept of fine-structured large deviations that leads to a periodic modulation of the probability distribution for displacements of stochastic motion along periodic substrates. It explains the deviations from a constant slope in an FT-like representation of this distribution, which are characteristic for systems with hidden degrees of freedom. Applied to molecular motors, our approach reveals how to infer entropy production from the properly discretized slope provided there are no idle cycles. The mean force exerted by a motor, however, is not related to such a long-time characteristics but rather given by the corresponding short-time limit. The application of these concepts to driven or active colloidal motion along a periodic structure will be left for future work.

* * *

We thank S. Toyabe for valuable interactions.

REFERENCES

[1] Seifert U., *Rep. Prog. Phys.*, **75** (2012) 126001.
[2] Jülicher F. *et al.*, *Rev. Mod. Phys.*, **69** (1997) 1269.
[3] Kolomeisky A. B. and Fisher M. E., *Ann. Rev. Phys. Chem.*, **58** (2007) 675.
[4] Seifert U., *Europhys. Lett.*, **70** (2005) 36.
[5] Andrieux D. and Gaspard P., *Phys. Rev. E*, **74** (2006) 011906.
[6] Astumian R. D., *Phys. Rev. E*, **76** (2007) 020102.
[7] Lau A. W. C. *et al.*, *Phys. Rev. Lett.*, **99** (2007) 158102.
[8] Lacoste D. *et al.*, *Phys. Rev. E*, **78** (2008) 011915.
[9] Lacoste D. and Mallick K., *Phys. Rev. E*, **80** (2009) 021923.
[10] Ge H., *J. Phys. A Math. Theor.*, **45** (2012) 215002.
[11] Hayashi K. *et al.*, *Phys. Rev. Lett.*, **104** (2010) 218103.
[12] Hayashi K. and Hayashi R., *Fluctuation and Noise Letters*, **11** (2012) 1241001.
[13] Hayashi K. *et al.*, *Eur. Phys. J. E*, **36** (2013) 136.
[14] Rahav S. and Jarzynski C., *J. Stat. Mech.: Theor. Exp.* (2007) P09012.
[15] Puglisi A. *et al.*, *J. Stat. Mech.: Theor. Exp.* (2010) P05015.
[16] Mehl J. *et al.*, *Phys. Rev. Lett.*, **108** (2012) 220601.
[17] Esposito M., *Phys. Rev. E*, **85** (2012) 041125.
[18] Altaner B. and Vollmer J., *Phys. Rev. Lett.*, **108** (2012) 228101.
[19] Touchette H., *Phys. Rep.*, **478** (2009) 1.
[20] Zimmermann E. and Seifert U., *New J. Phys.*, **14** (2012) 103023.
[21] Toyabe S. *et al.*, *Phys. Rev. Lett.*, **104** (2010) 198103.
[22] Toyabe S. *et al.*, *EPL*, **97** (2012) 40004.
[23] Lipowsky R., *Phys. Rev. Lett.*, **85** (2000) 4401.
[24] Liepelt S. and Lipowsky R., *Phys. Rev. Lett.*, **98** (2007) 258102.
[25] Gaspard P. and Gerritsma E., *J. Theor. Biol.*, **247** (2007) 672.
[26] Qian H., *Annu. Rev. Phys. Chem.*, **58** (2007) 113.
[27] Müller M. J. I. *et al.*, *J. Stat. Phys.*, **133** (2008) 1059.
[28] Astumian R. D., *Biophys. J.*, **98** (2010) 2401.
[29] Seifert U., *Phys. Rev. Lett.*, **106** (2011) 020601.
[30] Golubeva N. and Imparato A., *Phys. Rev. E*, **88** (2013) 012114.
[31] van Kampen N. G., *Stochastic Processes in Physics and Chemistry* (North-Holland, Amsterdam) 1981.
[32] Lebowitz J. L. and Spohn H., *J. Stat. Phys.*, **95** (1999) 333.
[33] Yasuda R. *et al.*, *Cell*, **93** (1998) 1117.
[34] Nishizaka T. *et al.*, *Nat. Struct. Mol. Biol.*, **11** (2004) 142.
[35] Rondelez Y. *et al.*, *Nature*, **433** (2005) 773.
[36] Gebhardt J. C. M. *et al.*, *Proc. Natl. Acad. Sci. U.S.A.*, **103** (2006) 8680.
[37] Speck T. *et al.*, *EPL*, **79** (2007) 30002.
[38] Gomez-Solano J. R. *et al.*, *Phys. Rev. Lett.*, **103** (2009) 040601.
[39] Volpe G. *et al.*, *Soft Matter*, **7** (2011) 8810.
[40] Mehl J. *et al.*, *Phys. Rev. E*, **78** (2008) 011123.
[41] Dorosz S. and Pleimling M., *Phys. Rev. E*, **83** (2011) 031107.
[42] Speck T. *et al.*, *J. Stat. Mech.: Theor. Exp.* (2012) P12001.